Remote Sensing of Tropospheric Pollution from Space

Jack Fishman
NASA Langley Research Center, Hampton, VA

Kevin W. Bowman
Jet Propulsion Laboratory, Pasadena, CA

John P. Burrows
University of Bremen, Bremen, Germany

Kelly V Chance
Harvard-Smithsonian Center for Astrophysics, Cambridge, MA

David P. Edwards
National Center for Atmospheric Research, Boulder, CO

Randall V. Martin
Dalhousie University, Halifax, Nova Scotia, Canada
Harvard-Smithsonian Center for Astrophysics, Cambridge, MA

Gary A. Morris
Valparaiso University Valparaiso, IN

R. Bradley Pierce
NOAA/NESDIS/STAR, Madison, WI

Jerald R. Ziemke
NASA Goddard Space Flight Center, Greenbelt, MD

Jassim A. Al-Saadi
NASA Langley Research Center, Hampton, VA

Todd K. Schaack
University of Wisconsin, Madison, WI

Anne M. Thompson
Pennsylvania State University, State College, PA

Corresponding author address: Jack Fishman, Mail Stop 401A, NASA Langley Research Center, Hampton, VA 23681-2199 USA
e-mail: jack.fishman@nasa.gov

Satellite observations of tropospehric trace gases provide exciting insight into atmospheric composition but using such measurements for air quality purposes requires significantly better temporal resolution which is attainable by placing instruments in geostationary orbit.

ABSTRACT

We review the progress of tropospheric trace gas observations and address the need for additional measurement capabilities as recommended by the National Academy of Science (NAS, 2007). Tropospheric measurements from current and earlier instruments show pollution in the Northern Hemisphere as a result of fossil fuel burning and a strong seasonal dependence with the largest amounts of photochemically-generated ozone in summer. At low latitudes, where photon flux is stronger throughout the year, trace gas concentrations are driven by the abundance of the emissions, where the largest source, biomass burning, is readily seen in carbon monoxide measurements, but lightning and biogenic trace gases may also contribute to trace gas variability. Although substantive progress has been achieved in seasonal and global mapping of a few tropospheric trace gases, satellite trace-gas observations with considerably better temporal and spatial resolution are essential to forecasting air quality at scales required by policy-makers. The concurrent use of atmospheric composition measurements for both scientific and operational purposes is a new paradigm for the atmospheric chemistry community. The examples presented illustrate both the promise and challenge of merging satellite information with *in situ* observations in state-of-the-art data assimilation models.

1. Introduction

From a climate perspective, trace gas composition is a key indicator that human activity is responsible for processes collectively classified as Global Change. Keeling's long-term *in situ* record of carbon dioxide (CO_2) measurements from Mauna Loa initiated in 1957 (Keeling et al., 1976) illustrates clearly that fossil fuel combustion has altered the atmospheric radiation balance, contributing to global warming (IPCC, 2007). Because CO_2 is such a long-lived species in the atmosphere, systematic surface measurements from selected locations are sufficient information to understand the seasonal, secular behavior of CO_2.

From an atmospheric chemistry perspective, ozone (O_3) is the most important molecule in both the stratosphere and the troposphere. Satellite measurement of stratospheric O_3 and other important trace gases that play an integral role determining O_3 distribution and abundance in the stratosphere have a substantial heritage dating back to the 1970s. When the ozone-hole was discovered in the early 1980s (Farman et al., 1985), several instruments confirmed the balloon-borne ozone measurement of unprecedented low values. Subsequently, dozens of instruments on various satellites were launched by space agencies in the 1990s and 2000s, providing a significant legacy for future satellite measurements of atmospheric trace gases. These satellites include the SAGE series (Stratospheric Aerosol and Gas Experiment), the TOMS (Total Ozone Mapping Spectrometer) series, two GOME (Global Ozone Monitoring Experiment) instruments, UARS (Upper Atmosphere Research Satellite, 1991-2005), ENVISAT (2002-), and Aura (2004-).

The measurement of lower atmospheric trace-gas composition is considerably more challenging technically, but satellite observations have also provided a good depiction of the global distribution of several species that otherwise could not have been attained. The NASA Aura satellite is the most recently launched (2004) U.S. satellite dedicated to the measuring trace gases, but no missions explicitly focused on atmospheric composition are in NASA's portfolio beyond the lifetime of Aura which is expected to be early in the next decade.

Studying tropospheric trace gas measurements from space begins with pioneering work using instruments designed to examine the stratosphere. Moving to satellites of the past decade, we see that with the advent of instruments able to measure trace gases in the troposphere, a new perspective on the interaction between local, regional, and global-scale processes emerged. Markers for pollution sources are visible as never before, and pathways of intercontinental transport have helped define the concept of "chemical weather." Traditional meteorological models are expanding with chemical reactions to take advantage of ever-increasing computer capability and the potential to assimilate satellite trace gas observations. We conclude with a preview of research operational air quality forecasting products (Dabberdt et al., 2003; McHenry and Dabberdt, 2005) and provide a snapshot of the kind of measurements recommended in the National Academy of Science (NAS, 2007) report written to address the earth-observing community's needs for the next decade and beyond.

2. Tropospheric Trace Gas Measurements from Space

At lower altitudes, many of the standard techniques that can be used to derive information about the stratosphere by viewing the earth's limb (e.g., see Burrows, 1999;

Kaye and Fishman, 2003) cannot be used, and, therefore, nadir viewing is required. Several tropospheric trace species can also be present in significant quantities in the stratosphere so that altitude discrimination is also required. Key measurable trace gases that are prevalent in both the troposphere and the stratosphere include ozone as well as its most important precursor for *in situ* tropospheric production, nitrogen dioxide (NO_2). A few important trace gases present predominantly in the lower atmosphere with enough of a spectral signature that they can be observed from a space platform include carbon monoxide (CO), formaldehyde (HCHO), glyoxal (CHOCHO), sulfur dioxide, SO_2 and the long lived greenhouse gases carbon dioxide (CO_2) and methane (CH_4).

Tropospheric trace gas measurements from space were proposed as part of NASA's Nimbus-7 satellite that was to be launched in 1978. The Measurement of Air Pollution from Satellites (MAPS) instrument, a gas-filter correlation radiometer (GFCR), was designed to measure carbon monoxide, a species of tropospheric origin and a key player in the reactions of other trace gases through its reaction with the hydroxyl radical (Crutzen and Fishman, 1977; Thompson et al., 1992). In the early 1970s, the global sources of CO were being disputed in the literature (McConnell et al., 1971; Seiler, 1974), with some studies suggesting that natural sources (e.g. oxidation of methane and non-methane hydrocarbons) were an order of magnitude larger than anthropogenic emissions (NAS, 1975). A global survey of CO from space would determine the relative strengths of these sources. The then-fledgling Environmental Protection Agency would benefit by knowing whether the human component of CO was large enough that regulations on CO would improve air quality.

Unfortunately, when NASA's Nimbus-7 was launched in 1978, the MAPS instrument had been removed from the payload and it was modified as an instrument to fly routinely in the Space Shuttle Program that started in 1981. MAPS flew aboard the Space Shuttle four times between 1981 and 1994 (Reichle et al., 1999) providing "snapshots" of CO distributions. These initial glimpses of CO confirmed that CO was highest where human sources from industry and tropical fires dominated. The Measurement of Pollution in the Troposphere (MOPITT) instrument, also a GFCR, has been measuring CO from the Terra Satellite launched in 1999. MOPITT's relatively long-term record has been used to determine the impact of localized emissions on global air quality. Wildfires in North America and Siberia have been especially strong sources of CO (Lamarque et al., 2003; Edwards et al., 2004), causing drastic ecosystem changes and alterations to carbon balance over Earth's vegetated areas through removal of above ground biomass, transport of CO and CO_2 into the atmosphere, and altering the carbon uptake by ecosystems. The 2004 Alaskan wildfire season was the region's worst on record because of unusually warm and dry weather. In central Alaska and Canada's Yukon Territory, more than 11 million acres burned. The location of high CO values measured by MOPITT (Fig. 1) coincided with the location of fires and aerosol plumes seen by Moderate Resolution Imaging Spectroradiometer (MODIS) which flew on the same platform as MOPITT. Model analysis using these observations indicated that from June to August 2004, the fires were responsible for some 30 Tg of CO, roughly equivalent to the total U.S. anthropogenic CO emissions for the same period. Ground-level ozone increased by about 25% in the northern U.S. and by up to 10% in Europe (Pfister et al., 2005). From its first observations of immense CO plumes from forest and

grassland fires in Africa and South America that traveled as far as Australia, MOPITT has provided the community with a tool for studying pollution sources, chemistry and transport in detail.

The Atmospheric InfraRed Sounder (AIRS) instrument onboard the Aqua satellite (launched in 2002) is also capable of providing information about CO (McMillan et al., 2005). Some preliminary products are currently being developed to use this information in near-real-time to investigate sources of CO and transport patterns. Comparisons of the CO data from AIRS with concurrent MOPITT observations (Warner et al., 2007) show some promise of the use of these data, which have the advantage of providing near global coverage on a daily basis.

3. Tropospheric Trace Gas Information from Satellite Measurements Designed to Study the Stratosphere

One instrument aboard Nimbus-7, TOMS, was designed to produce global daily maps of total ozone so that stratospheric ozone depletion (a hypothesis in 1978) could be observed, quantified, and the processes leading to it understood (Molina and Rowland, 1974). Working on the principle of measuring backscattered ultraviolet (buv) radiation, TOMS primarily provided information about the distribution of ozone in the stratosphere since ~90% of the ozone in the atmosphere lies in this region (~15-55 km). The remaining ~10% is located in the troposphere and is separated by the tropopause, which is generally located at an altitude between 10 and 18 km and varies as a function of both latitude and time of year. In the tropics, the tropopause is located higher in the

atmosphere (16-18 km) than at middle latitudes, where its height can be as low as 6-8 km, or as high as 15-16 km, with higher altitudes generally found in the summer.

The amount of ozone in a column of air is expressed in Dobson Units (DU) where one DU has a value of 2.69×10^{16} molec. of ozone cm^{-2}. A representative amount of total ozone in the atmosphere is 300 DU, of which ~30 DU is in the troposphere. At middle latitudes, the synoptic distribution of total ozone is primarily determined by the larger-scale distribution of ozone within the stratosphere; in turn, these patterns on a daily basis generally follow the upper-level airflow with the polar jet often being the demarcation between higher stratospheric ozone polewards and lesser amounts at lower latitudes. At low latitudes, therefore, large-scale synoptic patterns of total ozone are often not definitive because of the much weaker pressure gradients generally present there. In Fig. 2, the monthly distribution of total ozone is depicted using a color scale where the total ozone features at middle and high latitudes are off scale for better visualization at low latitudes (Fishman et al., 1990). The general enhancement in total ozone found at low latitudes over the South Atlantic and adjacent continents are generally observed during austral spring (September-November). Furthermore, when compared with CO measurements from the first MAPS Shuttle flight in November 1981, a significant positive correlation was identified (Fishman et al., 1986).

The data depicted in Fig. 2, however, reflect total ozone measurements, of which only a relatively small percentage is found in the troposphere. At higher latitudes, meteorological activity is generally more vigorous, and persistent patterns over the period of a week or two are rare. Therefore, identification of enhanced ozone of tropospheric origin is difficult and quasi-persistent plumes from Europe and northern Asia would be

lost beneath the variable stratospheric ozone amounts that would overwhelm any persistent tropospheric enhancements in these regions. Thus, persistent ozone sources in the tropics offered the first indications that satellite information could be used to identify ozone pollution sources.

a. Extracting Tropospheric Ozone from Total Ozone Column Measurements

The first step in retrieving the amount and distribution of many important tropospheric trace gases through space-based observations such as TOMS is to find a method for separating the tropospheric and stratospheric components from the total ozone measurements. Before that methodology was developed, however, an important analysis was provided in Fishman and Larsen (1987) where SAGE ozone profiles were used to calculate the stratospheric column ozone (SCO), which showed that stratospheric ozone at low latitudes exhibited little longitudinal variability. TOMS measurements, on the other hand, between 15°N and 15°S showed that the distribution of total ozone was quite different from the SCO distribution and was generally highest over the south tropical Atlantic Ocean. Furthermore, the difference between the total column and the SCO was highly correlated with the total ozone measured by TOMS.

During the 1990s, a number of research groups focused on extracting information about the troposphere from satellite measurements by assuming that ozone variability in the stratosphere is defined on relatively large spatial scales compared with the troposphere and that information could be obtained about the troposphere if this larger scale stratospheric component could be isolated. Once the stratospheric ozone

distribution was determined, the "residual" information (tropospheric ozone residual, TOR) could be used to infer information about the troposphere (see Fig. 3).

Using standard tropopause height information from the National Center for Environmental Prediction (NCEP) in conjunction with the collocated TOMS total ozone and SAGE profiles, Fishman et al., (1990) produced the first climatological depiction of tropospheric ozone on a domain that included both the tropics and middle latitudes (~50˚ N to ~50˚ S). The seasonal climatology of the TOR showed elevated amounts of tropospheric ozone at northern temperate latitudes during the summer; elevated TOR values are also present in the tropics and subtropics in the Southern Hemisphere during austral spring, a consequence of widespread biomass burning during that time of the year. This somewhat surprising finding in the South Atlantic became the focus of a major field campaign in 1992, Transport and Atmospheric Chemistry near the Equator—Atlantic (Fishman et al., 1996).

Subsequent to the TOMS/SAGE-derived TOR being published in 1990, a number of other research groups employed other methodologies to independently calculate SCO values to derive a quasi-global TOR distribution (e.g., Thompson and Hudson, 1999). SCO distributions were derived from the Microwave Limb Scanner (MLS) and the Halogen Occultation Experiment (HALOE) profiles from the UARS satellite launched in 1991 (Ziemke et al., 1998) and the Solar Backscattered Ultraviolet (SBUV) profiles from Nimbus-7 and several subsequent NOAA operational satellites (Fishman et al., 2003), Fig. 4.

Other techniques used characteristics of the TOMS measurements alone to develop a means of constructing an independent SCO value using information about how

the TOMS made its total column measurement. Two of these techniques compare the amount of total ozone at locations that are affected by the presence of clouds with total ozone amounts nearby in cloud-free regions. The difference in the column amounts is then defined as the tropospheric column ozone (TCO), and furthermore, by having independent information about the height of the clouds, upper tropospheric ozone profiles can then be calculated (Ziemke et al., 1998; 2001). Somewhat similarly, techniques have been developed using a knowledge of the heights of nearby mountains to infer the TCO in the layer up to mountaintop height by comparing total ozone amounts at the mountain locations with total ozone measurements at nearby locations (Newchurch et al., 2001).

b. Direct measurement of tropospheric ozone

Direct determination of ozone profiles, including tropospheric ozone content, from nadir measurements in the UV and visible was developed for the Scanning Imaging Absorption Spectrometer for Atmospheric Chartography (SCIAMACHY) instrument on the European ENVISAT satellite by applying a retrieval algorithm for ozone using information from differential penetration into the atmosphere. An altitude dependence was then determined by fitting the absorption to the temperature-dependent ozone Huggins bands (Chance et al., 1991; 1997; Bhartia *et al*., 1996). The method was originally applied to GOME spectral measurements (Munro *et al*., 1998; Hoogen *et al*., 1999) and has now been used to determine a multi-year climatology of tropospheric ozone (Liu et al., 2005; 2006). SAGE also obtained direct measurements of ozone in the upper troposphere at low latitudes using an occultation technique when cumulus clouds are not present (Wang et al., 2006).

4. Tropospheric NO_2

Although significant quantities of nitrogen dioxide are found in both the stratosphere and the troposphere, the amount of NO_2 found in the atmosphere can vary by more than two orders of magnitude and nearly all of this variability takes place in the troposphere. Thus, when the total column amount of NO_2 significantly exceeds values of ~1 x 10^{15} molec. cm^{-2} at low and middle latitudes, the integrated column amount generally reflects the amount present in the troposphere. Tropospheric NO_2 columns have been retrieved independently from GOME, SCIAMACHY and the Ozone Monitoring Instrument (OMI) by several groups (Martin et al., 2002; Richter and Burrows, 2002; Beirle et al., 2003; Boersma et al., 2004; Bucsela et al., 2006). The retrieval involves three steps: (1) determining total NO_2 line-of-sight (slant) columns by spectral fitting of solar backscatter measurements, (2) removing the stratospheric columns by using data from remote regions where the tropospheric contribution to the column is small, and (3) applying an air mass factor (AMF) for atmospheric scattering to convert tropospheric slant columns into vertical columns. Accounting for scattering by clouds is of particular importance. The retrieval uncertainty is determined by steps 1 and 2 over remote regions where there is little tropospheric NO_2, and by step 3 over regions of elevated tropospheric NO_2 (Martin et al., 2002; Boersma et al., 2004).

Fig. 5 shows tropospheric NO_2 columns retrieved from SCIAMACHY. Pronounced enhancements are evident over major urban and industrial regions. The high degree of spatial heterogeneity provides empirical evidence that most of the tropospheric NO_2 column is concentrated in the lower troposphere and close to local emissions. As a

result, tropospheric NO_2 columns retrieved from satellite observations show considerable prospect for inferring surface nitrogen oxides (NO_x) emissions through inversion of the NO_2 observations (Leue et al., 2001; Martin et al., 2003; Jaeglé et al., 2005).

5. Formaldehyde

Formaldehyde was hypothesized to exist in ubiquitous quantities in Levy's (1971) classic paper of tropospheric photochemistry as an intermediate product of methane oxidation after reacting with the hydroxyl radical (OH). Background HCHO concentrations coming directly from CH_4 oxidation are too small to be observable from present-day satellites, but the oxidation of other volatile organic compounds (VOC) that react quickly with OH also produces large amounts of HCHO. Thus, HCHO serves as a major proxy for these species when they are present in relatively large quantities. Formaldehyde was first measured from GOME spectra during the intense biomass burning over Asia in 1997 (Thomas et al., 1998). Development of more sensitive measurement capabilities has led to a global HCHO climatology that is used to determine the distribution of VOC emissions (Chance et al., 2000; Abbot et al., 2003; Shim et al., 2005; Fu et al., 2007). Fig. 6 depicts the average HCHO distribution during August 2005 from OMI. The major source region over the U.S. is in the southeastern states where densely populated deciduous forests permeate the landscape. Although anthropogenic VOC emissions are also important for the generation of photochemical pollution, the HCHO depiction illustrates the dominance of the natural sources in this region. Recently, the glyoxal radical, CHOCHO, has been measured from space, using OMI and SCIAMACHY spectra (Kurosu et al., 2005); glyoxyl is another proxy for VOC sources

with shorter lifetimes and likely a better indicator of urban sources (Volkamer et al., 2005).

6. Providing Global Insight into Trends and Interannual Variability

As the data records extend to a decade or longer, important trend information about some emissions in specific regions of the world is now becoming available. For example, NO_2 measurements from the GOME and SCIAMACHY instruments have identified a rapid increase in tropospheric NO_2 columns over industrial China during the last decade confirming a dramatic increase in regional emissions (Richter et al., 2005). This same data set also shows that emissions have decreased over much of Europe and that trends in Japan and the United States were close to zero, or slightly downward over this time frame. From the analysis of long-term tropospheric ozone column measurements using the multi decadal record of TOMS, several studies have suggested that the tropospheric ozone column has increased since the early 1980s (Ziemke et al., 2005; Jiang and Yung, 1996).

The 7-year MOPITT data set now provides a global record of the recent interannual variability of tropospheric air quality which is greater than previously thought due to large fire emissions being affected by climatic conditions that control rainfall and vegetation drying (Fig. 7). These data form the foundation of a long-term observational record that is used to investigate links among chemistry, climate, and other components of the Earth system (Edwards et al., 2003; 2004; Yurganov et al., 2005). For example, strong correlations have been observed between Southern Hemisphere CO zonal average loading,

fire activity in Indonesia and El Niño conditions (Edwards et al., 2006).

Also, because of the robust nature of the TOMS data record, regional interannual variability of tropospheric ozone has been linked to the El Niño/Southern Oscillation in both western Africa and northern India (Fishman et al., 2005). As seen in Fig. 8, considerably more tropospheric ozone is present in northeastern India in June during an "El Niño" year (1982) than over the same region during a "La Niña" year (1999). The primary reason for this is the delay of the onset of the summer monsoon during El Niño years, thereby providing more favorable conditions for the photochemical generation of ozone pollution throughout the entire month.

7. Tropospheric Measurements from Aura

With the launch of Aura in 2004, an entire satellite was launched devoted to atmospheric chemistry. The Tropospheric Emission Spectrometer (TES), a Fourier transform spectrometer whose heritage traces back to the InfraRed Interferometer Spectrometer (IRIS) aboard the Nimbus 4 spacecraft (Hanel and Conrath, 1969), provides simultaneous observations of CO and tropospheric O_3 vertical profiles (Beer, 2001). Simultaneous observations of these two species are particularly valuable for distinguishing between natural and anthropogenic sources of ozone (Fishman and Seiler, 1983). The spatial and vertical information from these measurements is critical for understanding the complex interplay between dynamics and chemistry that determines the global distribution of ozone. The value of concurrent measurements is further enhanced through data assimilation tools that are still in the developmental stage. An

example of the progress that has been made in this research arena is described subsequently.

Using the Aura data, Ziemke et al. (2006) derived TOR distributions by subtracting MLS SCO from OMI total column ozone. Although the OMI/MLS TOR data record is relatively short, it was used to study the effects of the tropical 1to 2 month Madden-Julian Oscillation on tropospheric ozone during the El Niño event in 2004 (Ziemke et al., 2006). Schoeberl et al. (2007, unpublished data) and Fishman et al. (2007, unpublished data) are both using information from models to derive SCO fields that are subtracted from OMI total ozone fields to derive a quasi-global TOR product.

A preliminary validation of these three different approaches to TOR calculation using data from Aura shows that there is generally good agreement between the derived products and the ozonesondes launched during overpasses. Some differences are due, at least in part, to non-uniform tropopause height definitions between the three approaches. Fig. 9 shows the time series of TOR data from the three techniques along with integrated ozonesonde data from a sample of two stations: one in the southeastern U.S. and one near the tropospheric ozone maximum found during September-November in the South Atlantic. In general, all three techniques reproduce the observed seasonal cycles and perform better in the tropics than at mid or high latitudes, where they notably fail to capture the day-to-day variability observed in the ozonesondes. Tropopause definition significantly impacts the result, so it will be important to establish a consistent tropopause definition for validation and evaluation of future TOR products.

With the capability to discriminate more than one layer in the troposphere, observations from TES have provided new insight into how the ozone maximum found

off the west coast of Africa (Fishman et al., 1990; 1996) evolved. Subsequent to its discovery using satellite data, *in situ* observations from ship cruise campaigns (Thompson et al., 2000) and model studies (Edwards et al., 2003; Martin et al., 2002) showed that the early-year tropospheric ozone distribution over the tropical Atlantic Ocean is characterized by two maxima: one in the lower troposphere north of the Intertropical Convergence Zone (ITCZ) and one in the middle and upper troposphere south of the ITCZ. This feature could not be resolved from initial analysis using only buv measurements. In Jourdain et al., 2007, TES vertical ozone retrievals provided the first space-based observations that characterized this complex altitude-dependent interplay between chemistry and transport. In particular, an enhanced layer of O_3 was observed by TES below 600 hPa that was advected by Harmattan winds from burning over western and central Africa.

In Zhang et al., 2006, correlations from simultaneous observations of CO and ozone from TES were used to investigate the export of pollution from continental outflow regions in the middle troposphere. Significant positive correlations ($R > 0.4$) were observed downwind of the eastern United States and east Asia, and over central Africa with ozone to CO enhancement ratios between 0.4 and 1.0, providing additional insight into the role that long-range transport plays on the observed global distribution of tropospheric ozone.

8. Data Assimilation, Air Quality, and the Development of Information with Better Temporal and Spatial Resolution

Data assimilation provides a statistically robust means of blending information from model predictions (or “first guess”) and different sets of observations at different

times to yield a physically consistent representation of the observed atmospheric state at synoptic intervals. The analysis is constructed by applying an analysis increment, based on the differences between a model first guess and observations, to the first guess to obtain an improved estimate of the true state of the atmosphere. The availability of validated MOPITT data motivated several advances in data assimilation of satellite trace gas measurements into chemical transport models. Data assimilation also facilitates comparison of satellite measurements with correlative data, especially when there is not an exact coincidence in time and location (Lamarque et al., 2004: Yudin et al., 2004).

With the launch of Aura in 2004, an expanded data-assimilation effort to produce consistent three-dimensional maps of several tropospheric trace gases was initiated using a chemical transport model with stratospheric heritage (Pierce et al., 1994). The chemical modeling/assimilation tool used in the example that follows is from the NASA Langley Research Center/University of Wisconsin (LaRC/UW) Regional Air Quality Modeling System (RAQMS; Pierce et al., 2003; 2007). The assimilation of column ozone observations provides an overall constraint on total column ozone, while the assimilation of profile retrievals constrains lower stratospheric and tropospheric O_3 and CO.

The RAQMS meteorological forecasts are initialized from NOAA's Global Forecast System (GFS) analyses at 6-hour intervals and the RAQMS OMI column assimilation, which likewise occurs at 6-hour intervals. The RAQMS TES O_3 and CO assimilation occurs at 1-hour intervals using the averaging kernel and *a priori* provided in the TES Level-2 (L2) data product. Estimates of the RAQMS forecast error variances are calculated by inflating the analysis errors (a by-product of the analysis) using the error growth model of Savijarvi (1995).

Fig. 10 shows composite comparisons between RAQMS O_3 and CO analyses and coincident TES special step and stare (SS) observations taken over the continental U.S. during August 2006. The TES SS observations were not assimilated and therefore provide an independent set of measurements for evaluating the fidelity of the RAQMS assimilation. Comparison between TES and RAQMS O_3 and CO analyses with the TES averaging kernel and *a priori* applied (not shown) shows mean differences of less than 10% for O_3 and 10 to 20% for CO. Both RAQMS O_3 and CO analysis (with TES observation operator applied) tend to be low relative to the TES SS data over the U.S.

TES SS and RAQMS composites show similar distributions, although the RAQMS composite shows more meridional continuity in both O_3 and CO than the TES SS composite due to the influence of the relatively coarse latitudinal variation in the TES *a priori* information on the retrieval. Both composites show significant (>80 ppbv) O_3 enhancements in the upper troposphere. The subtropical upper tropospheric O_3 enhancements are associated with low CO mixing ratios in both the TES SS and RAQMS composites implying significant stratospheric influences. Low level ozone enhancements of 60 to 80 ppbv between 30°N to 40°N are associated with CO mixing ratios of 120 to 160 ppbv in both the TES SS and RAQMS composites implying photochemical ozone production within the continental U.S. boundary layer. Both composites show mid-latitude upper tropospheric O_3 enhancements that are associated with moderate CO mixing ratios, suggesting a complicated mixture of both stratospherically influenced and polluted air in this region.

Daily ozonesonde launches, in support of the NOAA TexAQS field mission, were conducted throughout the continental U.S. during August 2006 as part of the

Intercontinental Chemical Transport Experiment Ozonesonde Network Study (IONS) program (Thompson et al., 2007). A total of 373 ozonesonde profiles during this time period provide an unprecedented opportunity to evaluate the quality of the RAQMS ozone analysis. Fig. 11 shows the August mean RAQMS analyzed tropospheric O_3 and total CO columns along with comparisons between RAQMS and IONS O_3 and RAQMS and MOPITT CO for selected IONS sites. Mean MOPITT CO profiles at the IONS ozonesonde sites were obtained by compositing all daytime MOPITT observations within 1^o of the IONS site during August, 2006.

The analyzed tropospheric ozone column shows a broad maximum in excess of 50 DU over the South central and eastern U.S. that extends out over the Western Atlantic and a localized ozone maximum off the California coast. The analyzed total column CO shows a similar CO maximum over the South central and eastern U.S. but no significant CO enhancement off the California coast. The collocated tropospheric O_3 and CO enhancements are due to photochemical ozone production and emissions associated with power generation facilities located east of the Mississippi and large urban centers along the Great Lakes and northeastern U.S. The tropospheric O_3 enhancements without significant CO enhancements are due to accumulation of stratospherically influenced air within the persistent subtropical high-pressure system off the California coast.

9. The Research-to-Applications Paradigm for Air Quality

The 2006 INTEX-B integrated satellite/aircraft campaign to investigate the transport and transformation of pollution from Asia to North America partnered with the TexAQS-2006 campaign to study the effects of distant and local sources on air quality in

Texas. The study provides an exciting set of opportunities to investigate global and regional impacts of air quality using a variety of space borne sensors. The integration of these measurements with *in-situ* data, models, and assimilation techniques is yielding rich gains in our understanding of air quality (http://www.espo.nasa.gov/intex-b/index.html; http://esrl.noaa.gov/csd/2006/). As promoted by the National Research Council (NRC) decadal survey (NAS, 2007) this approach is a new paradigm for air quality prediction following the pioneering efforts of the weather forecast community.

The successful involvement of both scientific and operational agencies in this process is examined through research that is focused on how applications are most usefully transmitted into operational domains. With respect to atmospheric composition, the first operational products have become a reality in recent years (Al-Saadi et al., 2005; http://idea.ssec.wisc.edu/; http://airnow.gov/). This information is used to advise people to remain indoors if they are susceptible to respiratory stress when exposed to elevated levels of pollution. The use of future satellite technology to improve forecasts of detrimental aspects of air quality underlay the NAS recommendation that the next atmospheric composition mission needs to be from geostationary orbit.

10. Implementing the Decadal Survey Recommendation for Air Quality

The atmospheric chemistry/composition community has traditionally not been faced with the challenge of using tropospheric trace species measurements in forecast mode and it was clear in the NAS report that the tools currently do not exist to use such information. The most obvious missing piece is the lack of sufficient temporal

resolution. An example of this shortcoming is shown in Fig. 12 and summarizes model results and measurements obtained during an Aura validation campaign June 22 & 23, 2005. The two OMI NO_2 column measurements over Houston are depicted by the red circles on the plot and were made at ~1900 on each day; the distribution at the time of the measurement for the two days is shown in the center and right panels above the plots. The left top panel shows the NO_2 column distribution calculated with the Community Multi-scale Air Quality (CMAQ) model (Byun et al., 1999). On the hourly plot, there are two sets of calculated quantities: surface NO_2 concentration (magenta) and integrated tropospheric NO_2 (dark blue), the quantity being measured by OMI. For NO_2, because its distribution is dominated by local sources (see Fig. 5), the quantity observed by the satellite is closely linked to its concentration at the surface. Furthermore, the diurnal behavior of these quantities is also closely linked. If an instrument like OMI were in geostationary orbit, technology already exists that can provide hourly observations of the type indicated by the blue diamonds during daylight hours, which are signified by the yellow background shading. Thus, an instrument using today's technology that "stares" at a region throughout the course of the day captures the most significant part of the diurnal variability that is totally missed by the low-earth orbiting Aura platform measuring values of 8 and 4 x 10^{15} molec. cm^{-2}, for the 22nd and 23rd, respectively.

To improve on the ability to measure ozone in the lower atmosphere, and especially near the surface, important advances in instrument capability may also be needed (Edwards, 2006). Recently, Worden et al. (2007) showed the potential of combining UV and IR spectral radiances from both TES and OMI in a unified retrieval algorithm with significantly improved sensitivity in the troposphere. This approach may

lay the groundwork for a new class of instruments that incorporate wavelengths across the ultraviolet, visible, and infrared spectrums that could revolutionize our observational capability from space of CO and O_3 within the planetary boundary layer and usher in a new era of air quality forecasting and prediction.

Regardless of the instrumentation that eventually resides in geostationary orbit to provide condtinuous high resolution measurements of tropospheric trace gases (and aerosols), a substantial challenge also awaits the general atmospheric chemistry/composition community to develop the mathematical tools that use this information. This point was emphasized in the Integrated Global Atmospheric Chemistry Observations strategy (Barrie et al., 2004), which cited the multi-pronged necessity of a strong modeling component as part of an integrated approach that will provide insight into tropospheric chemical and transport processes. Additionally, the modeling component will serve as the foundation for the eventual development of a robust air-quality forecasting capability. As part of Global Earth Observation System of Systems (GEOSS) <http://www.epa.gov/geoss/>, the satellite system of measurements needs to be integrated with data from ground-based observational (atmospheric composition) sites to develop a seamless three-dimensional field that can be used for both research and operational purposes. However, as pointed out by the air quality/atmospheric chemistry satellite science community (Edwards, 2006), the biggest piece missing in this grandiose scheme is the type of measurement capability that can be obtained only from a geostationary satellite and the NAS provided a roadmap that recommends such a mission in the 2013-2016 timeframe.

As outlined previously, the technology, although it can be improved upon, basically already exists and was successfully demonstrated from low-earth orbiting platforms. From the traditional meteorological perspective, the use of satellite information made a quantum advance when sensors were placed upon geostationary platforms. It is likely that similar quantum advancements will be realized when sensors devoted to atmospheric composition measurements are likewise put on a geostationary platform.

References

Abbot, D.S., P.I. Palmer, R.V. Martin, K. Chance, D.J. Jacob, and A. Guenther, Seasonal and interannual variability of North American isoprene emissions as determined by formaldehyde column emissions from space, 2003*: Geophys. Res. Lett*. **30**, 1886, doi:10.1029/2003GL017336.

Al-Saadi, J., J. Szykman, R.B. Pierce, C. Kittaka, D. Neil, D.A. Chu, L. Remer, L. Gumley, E. Prins, L. Weinstock, C. MacDonald, R. Wayland, F. Dimmick, and J. Fishman, 2005: Improving national air quality forecasts with satellite aerosol observations, *Bull. Amer. Meteor. Soc.*, **86**, 1249-1261.

Barrie, L.A., Borrell, P., and Langen, J., eds., 2004, *The Changing Atmosphere, an Integrated Global Atmospheric Chemistry Observation (IGACO) Theme for the IGOS Partnership,* Global Atmospheric Watch Rpt. 159 (World Meteorological TD No. 1235), 54 pp., Geneva

Bell, M. L., A. McDermott, S. L. Zeger, J. M. Samet, and F. Dominici, 2004: Ozone and short-term mortality in 95 U.S. urban communities, *J. Amer. Med. Assoc*., **292**, 2372-2378.

Beer, R., T. Glavich, and D. Rider, 2001: Tropospheric Emission Spectrometer for the Earth Observing System's Aura satellite. *Appl. Opt.*, **40**, 2356–2367.

Bhartia, P.K., R.D. McPeters, C.L. Mateer, L.E. Flynn, and C. Wellemeyer, 1996: Algorithm for the estimation of vertical ozone profiles from the backscattered ultraviolet technique, *J. Geophys. Res*. **101**, 18,793-18,806.

Beirle, S., U. Platt, M. Wenig, and T. Wagner, 2003: Weekly cycle of NO_2 by GOME measurements: A signature of anthropogenic sources, *Am. Chem. Phys.*, **3**, 2225-2232.

Boersma, K.F., H.J. Eskes, and E.J. Brinksma, 2004: Error analysis for tropospheric NO_2 retrieval from space, *J. Geophys. Res.*, **109**, D04311, doi:10.1029/2003JD003962.

Burrows, J.P., 1999: Current and future passive remote sensing techniques used to determine atmospheric constituents, in A.F. Bouwman (ed.), *Approaches to Scaling of Trace Gas Fluxes in Ecosystems*, Elsevier, Amsterdam, 317-347.

Bucsela, E.J., E.A. Celarier, M.O. Wenig, J.F. Gleason, J.P. Veefkind, K.F. Boersma, and E.J. Brinksma, 2006: Algorithm for NO_2 vertical column retrieval from the ozone monitoring instrument, *IEEE Trans. Geosci. Remote Sens.*, 44, 1245-1258.

Byun, D.W., and J.K.S. Ching, eds., 1999: Science algorithms for the EPA Models-3 Community Multiscale Air Quality (CMAQ) Modeling System, EPA-600/R-99/30.

Chance, K.V., J.P. Burrows, and W. Schneider, 1991: Retrieval and molecule sensitivity studies for the Global Ozone Monitoring Experiment and the SCanning Imaging Absorption spectroMeter for Atmospheric CHartographY, *Proc. S.P.I.E. Remote Sensing of Atmospheric Chemistry,* **1491**, 151-165.

Chance, K.V., J.P. Burrows, D. Perner, and W. Schneider, 1997: Satellite measurements of atmospheric ozone profiles, including tropospheric ozone, from UV/visible measurements in the nadir geometry: A potential method to retrieve tropospheric ozone, *J. Quant. Spectrosc. Radiat. Transfer,* **57**, 467-476.

Chance, K. P.I. Palmer, R.J.D. Spurr, R.V. Martin, T.P. Kurosu, and D.J. Jacob, 2000: Satellite observations of formaldehyde over North America from GOME, *Geophys. Res. Lett*. **27**, 3461-3464.

Crutzen, P. J., and J. Fishman, 1977: Average Concentrations of OH in the Northern Hemisphere and the Budgets of CH_4, CO, and H_2. *Geophys. Res. Lett.,* **4**, 321-324.

Dabberdt, W.F., et al., 2003: Meteorological research needs for improved air quality forecasting, *Bull. Amer. Metero. Soc.,* **84**, 563-585.

Edwards, D.P., 2006, Air quality remote sensing from space. *EOS, Transactions*, *Amer. Geophys, Union*, **87**, 327, doi:10.1029/2006EO330005.

Edwards, D. P., J.-F. Lamarque, J. -L. Attié, L. K. Emmons, A. Richter, J.-P. Cammas, J. C. Gille, G. L. Francis, M. N. Deeter, J. Warner, D. Ziskin, L. V. Lyjak, J. R. Drummond, and J. P. Burrows, 2003: Tropospheric ozone over the tropical Atlantic: A satellite perspective, *J. Geophys. Res*., **108**, 4237, doi:10.1029/2002JD002927.

Edwards, D. P., L. K. Emmons, D. A. Hauglustaine, A. Chu, J. C. Gille, Y. J. Kaufman, G. Pétron, L. N. Yurganov, L. Giglio, M. N. Deeter, V. Yudin, D. C. Ziskin, J. Warner, J.-F. Lamarque, G. L. Francis, S. P. Ho, D. Mao, J. Chan, and J. R. Drummond, 2004, Observations of Carbon Monoxide and Aerosol From the Terra Satellite: Northern Hemisphere Variability, *J. Geophys. Res.,* **109**, D24202, doi:10.1029/2004JD0047272004.

Edwards, D. P., G. A. Pétron, P. C. Novelli, L. K. Emmons, J. C. Gille, and J. R. Drummond, 2006: Southern Hemisphere carbon monoxide interannual variability observed by Terra/Measurement of Pollution in the Troposphere (MOPITT*), J. Geophys. Res.,* **111**, D16303 doi:10.1029/2006JD007079.

Farman, J.C., B.G. Gardiner, and J.D. Shanklin, 1985: Large loses of total ozone in Antarctica reveal seasonal ClO_x/NO_x interaction, *Nature,* **315**, 207-210.

Fishman, J., and J.C. Larsen, 1987: The distribution of total ozone and stratospheric ozone in the tropics: Implications for the distribution of tropospheric ozone. *J. Geophys. Res***., 92,** 6627-6634.

Fishman, J., and W. Seiler, 1983: Correlative nature of ozone and carbon monoxide in the troposphere: Implications for the tropospheric ozone budget, *J. Geophys. Res.,* **88**, 3662-3670.

Fishman, J. P. Minnis, and H.G. Reichle, Jr., 1986: Use of satellite data to study trace gas emissions in the tropics. *J. Geophys. Res.,* **91**, 14451-14465.

Fishman, J., C.E. Watson, J.C. Larsen, and J.A. Logan, 1990: Distribution of tropospheric ozone determined from satellite data. *J. Geophys. Res.,* **95,** 3599-3617.

Fishman, J., J.M. Hoell, Jr., R.D. Bendura, V.W.J.H. Kirchhoff, and R.J. McNeal, 1996: The NASA GTE TRACE-A experiment (September-October, 1992): *J. Geophys. Res.,* **101,** 23,865-23,879.

Fishman, J., A.E. Wozniak, and J.K. Creilson, 2003: Global distribution of tropospheric ozone from satellite measurements using the empirically corrected tropospheric ozone residual technique: Identification of the regional aspects of air pollution, *Atmos. Chem. Phys.,* **3**, 893-907, (www.atmos-chem-phys.org/acp/3/893/).

Fishman, J., J.K. Creilson, A.E. Wozniak, and P.J. Crutzen The interannual variability of stratospheric and tropospheric ozone determined from satellite measurements, 2005: *J. Geophys. Res.*, **110**, D20306, doi:10.1029/2005JD005868.

Fu, T.-M., D.J. Jacob, P.I. Palmer, K. Chance, Y.X. Wang, B. Barletta, D.R. Blake, J.C. Stanton, and M.J. Pilling, 2007: Space-based formaldehyde measurements as constraints on volatile organic compound emissions in East and South Asia, and implications for ozone,J. Geophys. Res. 2006JD007853R, (in press).

Hanel, R., and B. J. Conrath, 1969: Interferometer experiment on Nimbus 3: Preliminary results. *Science*, **165**, 1258.

Hoogen, R., V.V. Rozanov, and J.P. Burrows, 1999: Ozone profiles from GOME satellite data: Algorithm description and first validation, *J. Geophys. Res*. **104**, 8263–8280.

IPCC (Intergovernmental Panel of Climate Change, 2007), Climate Change **2007**: The Physical Science Basis. Summary for Policy Makers. www.**ipcc**.ch/SPM2feb07.pdf.

Jaeglé, L., L. Steinberger, R.V. Martin, and K. Chance, 2005: Global partitioning of NO_x sources using satellite observations: Relative roles of fossil fuel combustion, biomass burning and soil emissions, *Faraday Discussions*, **130**, 407-423, doi:10.1039/b502128f.

Jiang, Y. B. and Y. L. Yung, 1996: Concentrations of tropospheric ozone from 1979 to 1992 over tropical Pacific South America from TOMS data, *Science* **272,** 714-716.

Jourdain, L., H. M. Worden, J. R. Worden, K. Bowman, Q. Li, A. Eldering, S. S. Kulawik, G. Osterman, K. F. Boersma, B. Fisher, C. P. Rinsland, R. Beer, and M. Gunson, 2007: Tropospheric vertical distribution of tropical Atlantic ozone observed by TES during the northern African biomass burning season. *Geophys. Res. Lett.,* **34**, L04810, doi:10.1029/2006GL028284.

Kaye, J.A., and Fishman, J., Stratospheric Ozone Observations, 2003: in *Handbook of Climate, Weather, and Water: Chemistry, Impacts and Applications,* T.D. Potter and B. Colman, eds; Wiley, New York, 385-404.

Keeling, C.D., R.B. Bacastow, A.E. Bainbridge, C.A. Ekdahl, Jr., P.R. Guenther, L.S. Waterman, and J.F.S. Chin, 1976: Atmospheric carbon dioxide variations at Mauna Loa Observatory, Hawaii. *Tellus* **28**, 538-51.

Kurosu, T.P., K. Chance, and R. Volkamer, Global Measurements of OClO, BrO, HCHO, and CHO-CHO from the Ozone Monitoring Instruments on EOS Aura, Oral presentation #A54B-01, AGU Fall Meeting, 2005.

Lamarque, J.-F., D. P. Edwards, L. K. Emmons, J. C. Gille, O. Wilhelmi, C. Gerbig, D. Prevedel, M. N. Deeter, J. Warner, D. C. Ziskin, B. Khattatov, G. L. Francis, V. Yudin, S. Ho, D. Mao, J. Chen, and J. R. Drummond, 2003:, Identification of CO plumes from MOPITT data: Application to the August 2000 Idaho-Montana forest fires, *Geophys. Res. Lett.,* **30**, 1688, doi:10.1029/2003GL017503.

Lamarque, J.-F., B. Khattatov, V. Yudin, D. P. Edwards, J. C. Gille, L. K. Emmons, M. N. Deeter, J. Warner, D. C. Ziskin, G. L. Francis, S. Ho, D. Mao, and J. R. Drummond (2004), Application of a bias estimator for the improved assimilation of Measurements of Pollution in the Troposphere (MOPITT) carbon monoxide retrievals, *J. Geophys. Res.*, **109**, No. D16, D16304, doi:10.1029/2003JD004466.

Leue, C., M. Wenig, T. Wagner, O. Klimm, U. Platt, and B. Jahne, 2001: Quantitative analysis of NO_x emissions from GOME satellite image sequences, *J. Geophys. Res.*, **106**, 5493-5505.

Levy, H. II, 1971: Normal atmosphere: Large radical and formaldehyde concentrations predicted, *Science,* **173**, 141-143.

Liu, X., K. Chance, C.E. Sioris, R.J.D. Spurr, T.P. Kurosu, R.V. Martin, and M.J. Newchurch, 2005: Ozone profile and tropospheric ozone retrievals from Global Ozone Monitoring Experiment: Algorithm description and validation, *J. Geophys. Res.,* **110**, D20307, doi:10.1029/2005JD006240.

Liu, X., K. Chance, C.E. Sioris, T.P. Kurosu, R.J.D. Spurr, R.V. Martin, T.-M. Fu, J.A. Logan, D.J. Jacob, P.I. Palmer, M.J. Newchurch, I.A. Megretskaia, and R.B. Chatfield, 2006: First directly-retrieved global distribution of tropospheric column ozone from GOME: Comparison with the GEOS-CHEM model*, J. Geophys. Res.* **111**, D02308, doi:10.1029/2005JD006564.

Martin, R.V., et al.., 2002: An improved retrieval of tropospheric nitrogen dioxide from GOME, *J. Geophys. Res.*, **107**, 4437, doi:10.1029/2001JD001027.

Martin, R.V., D.J. Jacob, K. Chance, T.P. Kurosu, P.I. Palmer, and M.J. Evans, 2003: Global inventory of nitrogen oxide emissions constrained by space-based observations of NO_2 columns, *J. Geophys. Res.*, **108**, 4537, doi:10.1029/2003JD003453.

Mauzerall, D. L., and X. Wang, 2001: Protecting agricultural crops from the effects of tropospheric ozone exposure: Reconciling science and standard setting in the United States, Europe, and Asia, *Annul. Rev. Energy Environ.*, ***26***, 237-268.

McConnell, J.C., M.B. McElroy and S.C. Wofsy, 1971: Natural sources of atmospheric CO, *Nature,* **233**, 187-188.

McHenry, J.N., and W.F. Dabberdt, 2005: Air quality and meteorological monitoring strategies to advance air quality modeling and its application to operational air quality forecasting, Rept. EPA/600/R-05/154, 78 pp.

McMillan, W. W., C. Barnet, L. Strow, M. Chahine, M. McCourt, P. Novelli, S. Korontzi, E. Maddy, and S. Datta, 2005: Daily global maps of carbon monoxide: First views from NASA's Atmospheric Ifrared Sounder, *Gephys. Res. Lett.*, ***32*** (L11801), doi:10.1029/2004GL012,821.

Molina, M.J., and F.S. Rowland, 1974: Stratospheric sink for chlorofluoromethanes: chlorine atom catalyzed destruction of ozone, *Nature, **249***, 810-814.

Morgan, P. B., E. A. Ainsworth, and S. P. Long, 2003: How does elevated ozone impact soybean? A meta-analysis of photosynthesis, growth and yield, *Plant, Cell and Environ.*, **26**, 1317-1328.

Munro, R., R. Siddans, W.J. Reburn, and B. Kerridge, 1998: Direct measurement of tropospheric ozone from space, *Nature,* **392**, 168–171.

National Academy of Science, 1975: *Carbon Monoxide,* National Academy Press, Washington, DC 239 pp.

National Academy of Science, 2007: *Earth Science ad Applications from Space: National Imperatives for the Next Decade and Beyond*, National Academy Press, Washington DC (http://books.nap.edu/catalog.php?record_id=11820, in press).

Newchurch, M. J., X. Liu, J. H. Kim, 2001: Lower-Tropospheric Ozone (LTO) derived from TOMS near mountainous regions, *J. Geophys. Res.,* **106**, 20403-20412, 10.1029/2000JD000162.

Pfister, G. ,P.G. Hess, L.K. Emmons, J.-F. Lamarque, C. Wiedinmyer, D.P. Edwards, G. Pétron. J. C. Gille, and G.W. Sachse, 2005: Quantifying CO emissions from the 2004 Alaskan wildfires using MOPITT CO data, *Geophys. Res. Lett.,* **32**, L11809, doi:10.1029 /2005GL022995.

Pierce, R.B., W.L. Grose, and J.M. Russell, III, 1994: Evolution of Southern Hemisphere air masses observed by HALOE, *Geophys. Res. Lett.*, **21**, 213–216.

Pierce, R. B. et al., Regional Air Quality Modeling System (RAQMS) predictions of the tropospheric ozone budget over east Asia, 2003, *J. Geophys. Res*., **108**, 8825, doi:10.1029/2002JD003176.

Pierce, R. B., et al., (2007), Chemical data assimilation estimates of continental U.S. ozone and nitrogen budgets during the Intercontinenatal Chemical Transport Experiment—North America, *J. Geophys. Res*,, **112**, D12S21, doi:10.1029/2006JDoo7722.

Pope, C.A., 2000: Epidemiology of fine particulate air pollution and human health: biologic mechanisms and who's at risk? *Environ Health Perspect,* ***108*****,** 713–723.

Reichle, H.G., Jr. et al., 1999: Space shuttle based global CO measurements during April and October 1994, MAPS instrument , data reduction and data validation, *J. Geophys. Res.,* **104**, 21,443-21,454.

Richter, A., and J.P. Burrows, 2002: Tropospheric NO_2 from GOME measurements, *Adv. Space Res.*, **29**, 1673-1683.

Richter, A., J.P. Burrows, H. Nüß, C. Granier, and U. Niemeier, 2005: Significant increase in tropospheric nitrogen dioxide over China observed from space, *Nature*, **437**, 129-132, doi:10.1038/nature04092.

Savijarvi, H., 1995: Error growth in a large numerical forecast system. *Mon. Wea. Rev.* **123**, 212-221,

Seiler, W., 1974: The cycle of atmospheric CO, *Tellus,* **26**, 116-135.

Shim, C., Y. Wang, Y. Choi, P.I. Palmer, D.S. Abbot, and K. Chance, 2005: Constraining global isoprene emissions with GOME HCHO column measurements, *J. Geophys. Res*. **110**, D24301, doi:10.1029/2004JD005629.

Thomas, W., E. Hegels, S. Slijkhuis, R. Spurr, and K. Chance, 1998: Detection of biomass burning combustion products in South-east Asia from backscatter data taken by the GOME spectrometer, *Geophys. Res. Lett*., **25**, 1317-1320.

Thompson, A.M., 1992: The oxidizing capacity of the Earth's atmosphere: Probable past and future changes, *Science*, **256**, 1157-1165.

Thompson, A.M., and R.D. Hudson, 1999: Tropical tropospheric ozone (TTO) maps from Nimbus and Earth-Probe TOMS by the modified residual method: Evaluation with sondes, ENSO signals and trends from Atlantic regional time series, *J. Geophys. Res.,* **104**, 26961-26975.

Thompson, A.M., B. G. Doddridge, J. C. Witte, R. D. Hudson, W. T. Luke, J. E. Johnson, B. J. Johnson, S. J. Oltmans, and R. Weller. 2000: A tropical atlantic ozone paradox: Shipboard and satellite views of a tropospheric ozone maximum and wave-one in January – February 1999. *Geophys. Res. Lett.*, **27**, 3317–3320.

Thompson, A. M., et al., 2007: IONS (INTEX Ozonesonde Network Study, 2004): 1. Perspective on Summertime UT/LS (Upper Troposphere/Lower Stratosphere) Ozone over Northeastern North America, *J. Geophys. Res.,* **112**, D12S12, doi:10.1029/2006JD007441.

Volkamer, R., L.T. Molina, M.J. Molina, T. Shirley, and W.H. Brune, 2005: DOAS measurement of glyoxal as a new marker for fast VOC chemistry in urban air*, J. Geophys. Res*. **32**, L08806, doi:10.1029/2005GL022616.

Wang, P.-H., D.M Cunnold, C.R. Trepte, H.J. Wang, P. Jing, J. Fishman, V.G. Brackett, J.M. Zawodny and G.E. Bodeker, 2006: Ozone variability in the midlatitude upper troposphere and lower stratospshere diagnosed from a monthly SAGE II climatology relative to the tropopause, *J. Geophys. Res.,* **111**, D21304, doi:10.1029/2005JD006108.

Warner, J., M. McCourt Comer, D.D. Barnet, W.W. McMillan, W. Wolf, E. Maddy, and G. Sachse, 2007: A comparison of satellite tropospheric carbon monoxide measurements from AIRS and MOPITT during INTEX-A, *J. Geophys. Res.* **112**, D12S17, doi:10.1029/2006JD007925.

Worden, J., X. Liu, K. Bowman, K. Chance, R. Beer, A. Eldering, M. Gunson, and H. Worden. 2007: Improved tropospheric ozone profile retrievals using OMI and TES radiances, *Geophys. Res. Lett.*, **34,** L01809, doi:10.1029/2006GL027806.

Yudin, V., G. Pétron, J.-F. Lamarque, B. V. Khattatov, P. G. Hess, L. V. Lyjak, J. C. Gille, D. P. Edwards, M. N. Deeter, and L. K. Emmons, 2004:, Assimilation of the 2000-2001 CO MOPITT retrievals with optimized surface emissions, *Geophys. Res. Lett.,* **31**, L20105, doi:10.1029/2004GL021037.

Yurganov, L. N., P. Duchatelet, A. V. Dzhola, D. P. Edwards, F. Hase, I. Kramer, E. Mahieu, J. Mellqvist, J. Notholt, P. C. Novelli, A. Rockmann, H. E. Scheel, M. Schneider, A. Schulz, A. Strandberg, R. Sussmann, H. Tanimoto, V. Velazco, J. R. Drummond, J. C. Gille, 2005: Increased Northern Hemispheric carbon monoxide burden in the troposphere in 2002 and 2003 detected from the ground and from space, *Atm. Chem. and Phys*., **5,** 563-573.

Zhang, L., et al., 2006: Ozone-CO correlations determined by the TES satellite instrument in continental outflow regions, *Geophys. Res. Lett.*, **33**, 2006.

Ziemke, J. R., S. Chandra, and P. K. Bhartia, Two new methods for deriving tropospheric column ozone from TOMS measurements, 1998: The assimilated UARS MLS/HALOE and convective-cloud differential techniques, *J. Geophys. Res., **103**, 2*2,115-22,127.

Ziemke, J. R., S. Chandra, and P. K. Bhartia, 2001: “Cloud slicing": A new technique to derive upper tropospheric ozone from satellite measurements, *J. Geophys. Res*., **106**, 9853-9867.

Ziemke, J. R., S. Chandra, and P. K. Bhartia, 2005: A 25-year data record of atmospheric ozone from TOMS Cloud Slicing: Implications for trends in stratospheric and tropospheric ozone, J. Geophys. Res., 110, D15105, doi:10.1029/2004JD005687.

Ziemke, J. R., et al. (2006), Tropospheric ozone determined from Aura OMI and MLS: Evaluation of measurements and comparison with the Global Modeling Initiative's Chemical Transport Model, *J. Geophys. Res*., 111, D19303, doi:10.1029/2006JD007089

List of Figures

Western Russian fires in the late summer of 2002 and Siberian fires in the spring of 2003 produced so much CO that pollution built-up to produce a very "dirty winter."

Figure 8. Monthly distributions of TOR in DU during June 1982 ("El Niño year) and June 1999 (La Niña year).

Figure 9. Time series comparisons of the three different TOR techniques compared to ozonesonde data integrated from the surface to the World Meteorological Organization (WMO) tropopause. Red circles indicate ozonesonde observations at each location. The various colored points connected by a running average line indicate the TOR calculated by various techniques: Ziemke et al., 2006 (yellow); Schoeberl (blue); and Fishman (green)

Figure 10. Composite distribution of O_3 and CO over the continental U.S. during August 2006 based on TES step and stare observations (upper panels) and RAQMS coincident chemical analyses (lower panels).

Figure 11. Mean distribution of O_3 and CO over the continental US during August 2006. Upper panels show comparisons for Narraganset and Sable Island IONS sites. Lower panels show comparisons for Houston and Huntsville IONS sites. RAQMS (solid) and MOPITT (dashed) mean CO profiles and standard deviations are shown in red. RAQMS (solid) and IONS (dashed) mean O_3 profiles are shown in black. The IONS standard deviations are shown in green. The middle panels show the mean tropospheric column O_3 and total column CO based on six-hourly

RAQMS analyses. The location of the IONS sites are indicated by white diamonds with the selected sites labeled. The mean pressure of the analyzed thermal tropopause is contoured.

Figure 12. Two OMI NO_2 column measurements over Houston are depicted by the red circles at the time of the measurement (~1900 GMT) on June 22 and 23, 2005. The three depictions at the top portion of the figure are NO_2 column distributions: The left panel is calculated using CMAQ with a 12-km resolution; the other two panels are from OMI for the two respective days and all three depictions use the color scale above them. The diurnal calculations shown by the curves are the NO_2 surface concentrations (magenta) and the NO_2 columns (dark blue) calculated by the CMAQ model for Houston and are plotted hourly over this 2-day period. The yellow shading indicates daylight hours and illustrates when data using the solar backscattered technique (as used by OMI) could be obtained from a geostationary orbit.

Sidebar Figure. Schematic diagram of simplified tropopsheric photochemistry. Species in red can be measured using existing satellite instrumentation. CO, NO and VOCs are emitted in the planetary boundary layer from both anthropogenic and biogenic sources. NO_2 is rapidly converted in the troposphere from emitted NO and the two nitrogen oxides (NO_x) establish an equilibrium ratio between each other depending on a number of atmospheric variables such as the intensity of sunlight and the amount of O_3. HCHO is an intermediate product of VOC oxidation, and its measurement is a good indication of the amount of VOCs present. The amount of O_3 produced is directly proportional to how much NO_2 is present when sunlight is available (denoted by the "sun" symbol). Ozone can also be transported to the troposphere from the stratosphere where it is produced

naturally by the photolysis of molecular oxygen (O_2) because of high-energy photons in the upper atmosphere ($\lambda < 242$ nm) that are capable of breaking apart the O_2 molecule. Lightning is also a natural source of NO_x in the free troposphere.

The NAS Report

To appear as a Sidebar

In 2004, NASA, NOAA and the U.S. Geological Society (USGS) requested that the National Academy of Science (NAS) form a panel to identify and prioritize the next set of observational platforms that should be launched and operated over the next decade. In addition to providing information solely for the purpose of addressing scientific questions, the NAS took the approach that increasing the societal benefits of Earth science research should likewise be high on the priority list of federal science agencies and policymakers, who have long believed that the role of scientific research is not only to expand our knowledge but also to improve the lives of Americans.

For example, in the U.S. today, an estimated 1.8 to 3.1 years of life are lost to people living in the most polluted cities due to chronic exposure to particulates (Pope, 2000). In addition, more than 4000 premature deaths per year occur because of the elevated ozone concentrations now commonly observed in the U.S. (Bell et al., 2004). Elevated surface ozone concentrations also have deleterious effects on crop production/yield (Mauzerall and Wang, 2001; Morgan et al., 2003) costing U.S. agriculture more than a billion dollars annually.

The NAS emphasized that if Earth scientists are to foster applications and extend the societal benefits of their work, they must also understand the research to applications chain, which includes transforming satellite measurements into useful information and distributing that information in a form that is understandable and meets the needs of both public and private sector managers, decision-makers, and policy-makers.

Specifically, with respect to future atmospheric chemistry missions, the NAS (2007) recommended that a mission dedicated to the measurement of tropospheric trace

gases from a geostationary spacecraft should be launched in the 2013-2016 timeframe (GEO-CAPE, Geostationary Coastal and Air Pollution Events Mission) and that such a mission would fit into its vision of providing societal benefit. The NAS also called for another satellite similar to Aura to be launched again in the 2020 timeframe (Global Atmospheric Composition Mission, GACM).

The use of Earth science data for applications will first require gaining an understanding how research-level data can be used in a successful operational environment (NAS, 2007). Extracting societal benefit from space-borne measurements necessitates, as an equally important second step, the development of a strong link between the measurements and decision makers who will use such measurements. This linkage must be created and sustained throughout the lifecycle of the space mission. In order to implement future missions, scientists who are engaged in research intended to have both scientific and societal contributions must operate differently than they did in the days when the advancement of science was the primary or only goal of research. Applications development places new responsibilities on agencies to balance applications demands with scientific priorities and the character of missions may change in significant ways if societal needs are given equal priority with scientific needs. This potential societal benefit was interwoven into the foundation for the NAS requirement of making atmospheric composition measurements from a geostationary platform its highest priority. As this new paradigm evolves, the numbers of published papers, or scientific citation indices, or even professional acclamation from scientific peers, will not be enough to evaluate the success of the missions that have been recommended. The degree to which human welfare has been improved and the effectiveness of protecting property

and saving lives will additionally become important criteria for a successful Earth science and observations program.

Basic Tropospheric Chemistry

To appear as a Sibebar

Tropospheric ozone (O_3) is the central character that drives the chemistry of the lower atmsophere. From an atmospheric chemist's point of view, if the global distribution of tropospheric ozone and the evolution of that distribution are understood, then most of the primary questions driving the science can be answered. The primary challenge is the fact that ozone is both a natural and a man-made component of the lower atmosphere (as opposed to the stratosphere, where ozone is produced only naturally). The two major sources of O_3 are its transport from the huge stratospheric reservoir and its *in situ* photochemical production from the release of anthropogenic and biogenic precursors that are oxidized in the atmosphere to eventually become ozone. For the most part, most of these trace gases are initially oxidized by the hydroxyl (OH) radical and its abundance, and distribution, in turn, is most dependent on the O_3 present in the troposphere. Thus, if the distribution of O_3 is well known, then we can get a good handle on the oxidizing capacity of the atmosphere and the global extent of air pollution, two of the "grand challenges" put forth in the integrated global observations strategy for atmospheric composition (Barrie et al., 2004). Global observations of trace gases using satellites have already provided the community with a unique set of observations that have already yielded important insights by being able to measure CO, NO_2, HCHO and O_3, itself.

Tropospheric O_3 is formed when certain precursor trace gases are oxidized in the atmosphere by the OH radical. The two most important precursor trace gases are CO and a class of gases known as volatile organic carbon (VOC) species. However, the amount

of O_3 that forms is most critically dependent on the available concentration of nitrogen oxides (NO_x), which is primarily the sum of nitrogen oxide (NO) and nitrogen dioxide (NO_2). Putting it into a chemical reaction formulation, there are two potential pathways:

$$\text{VOC (or CO)} + \text{OH} + \text{sunlight} \rightarrow H_2O + CO_2 \text{ (no } NO_x\text{)} \quad [1]$$

$$\text{or} \quad \text{VOC (or CO)} + \text{OH} + \text{sunlight} \rightarrow \mathbf{O_3} + H_2O + CO_2 \text{ (with } NO_x\text{)}. \quad [2]$$

From satellites, we can measure formaldehyde, (HCHO, a surrogate for VOC), CO, O_3, and NO_2 (one of the two primary components of NO_x).

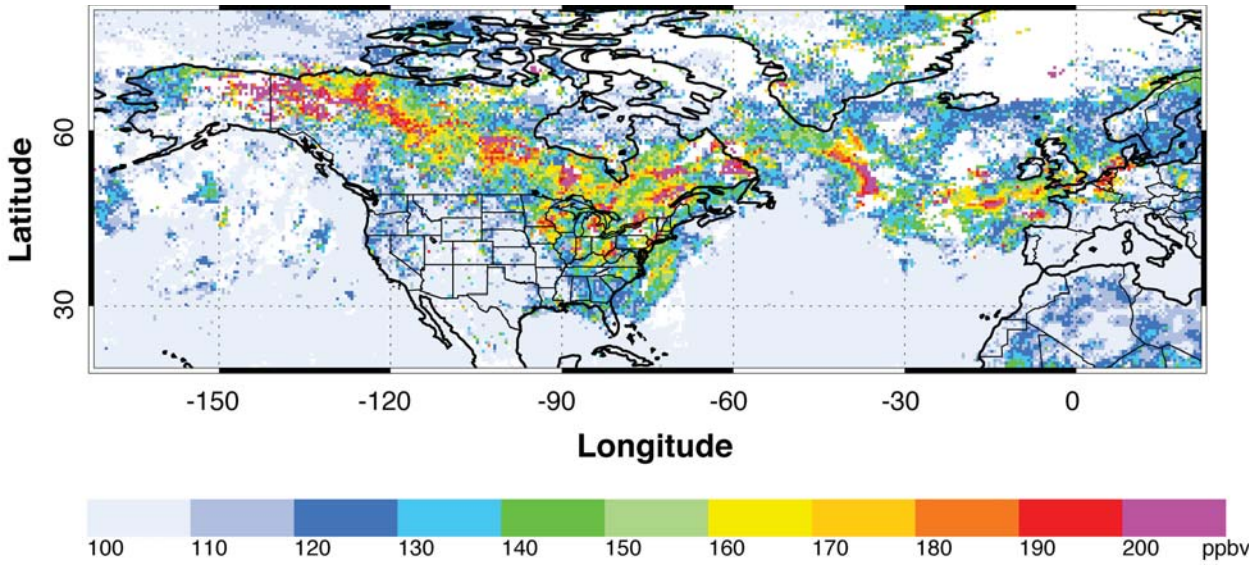

Figure 1: MOPITT 700 hPa CO mixing ratio for July, 15-23, 2004, during the INTEX-NA field campaign. The intense wildfires in Alaska produced plumes of pollution that can be traced across North America and the Atlantic Ocean.

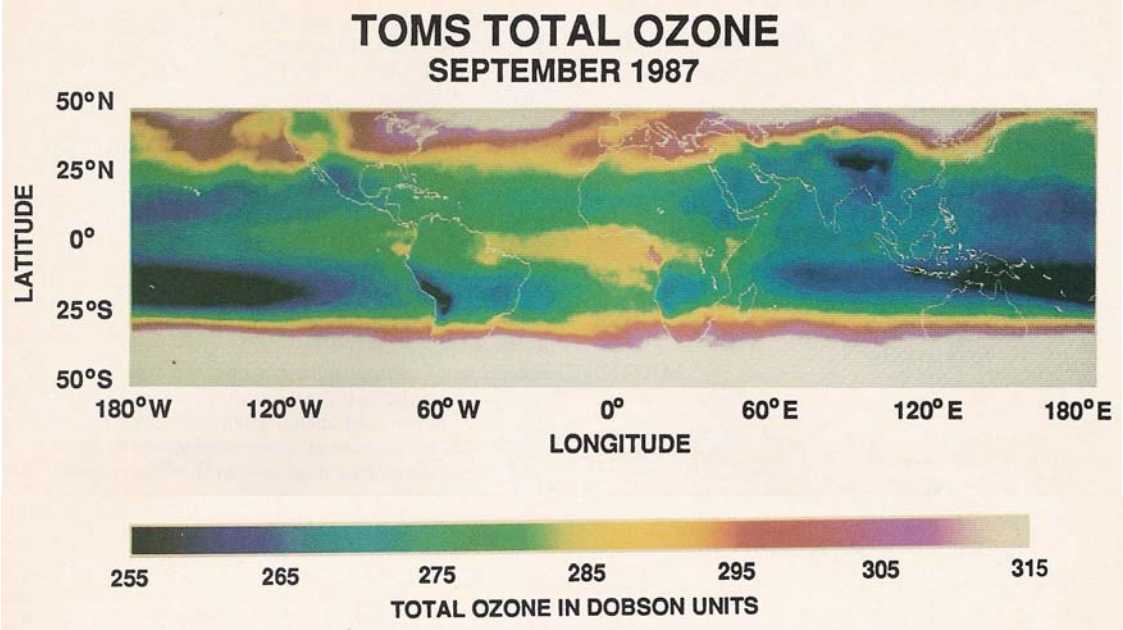

Figure 2. Total ozone distribution of for September 1987 as determined from the TOMS satellite (from Fishman et al., 1990).

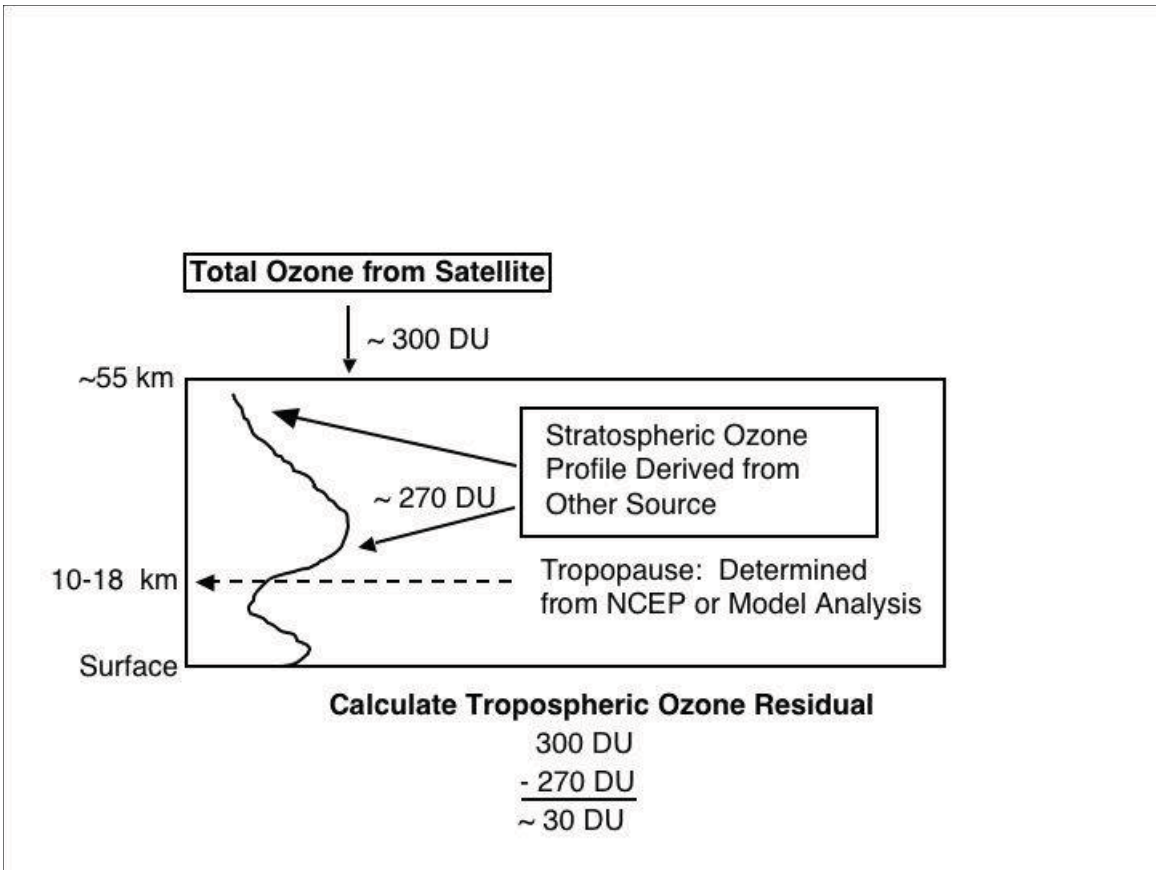

Figure 3. Schematic of the TOR technique.

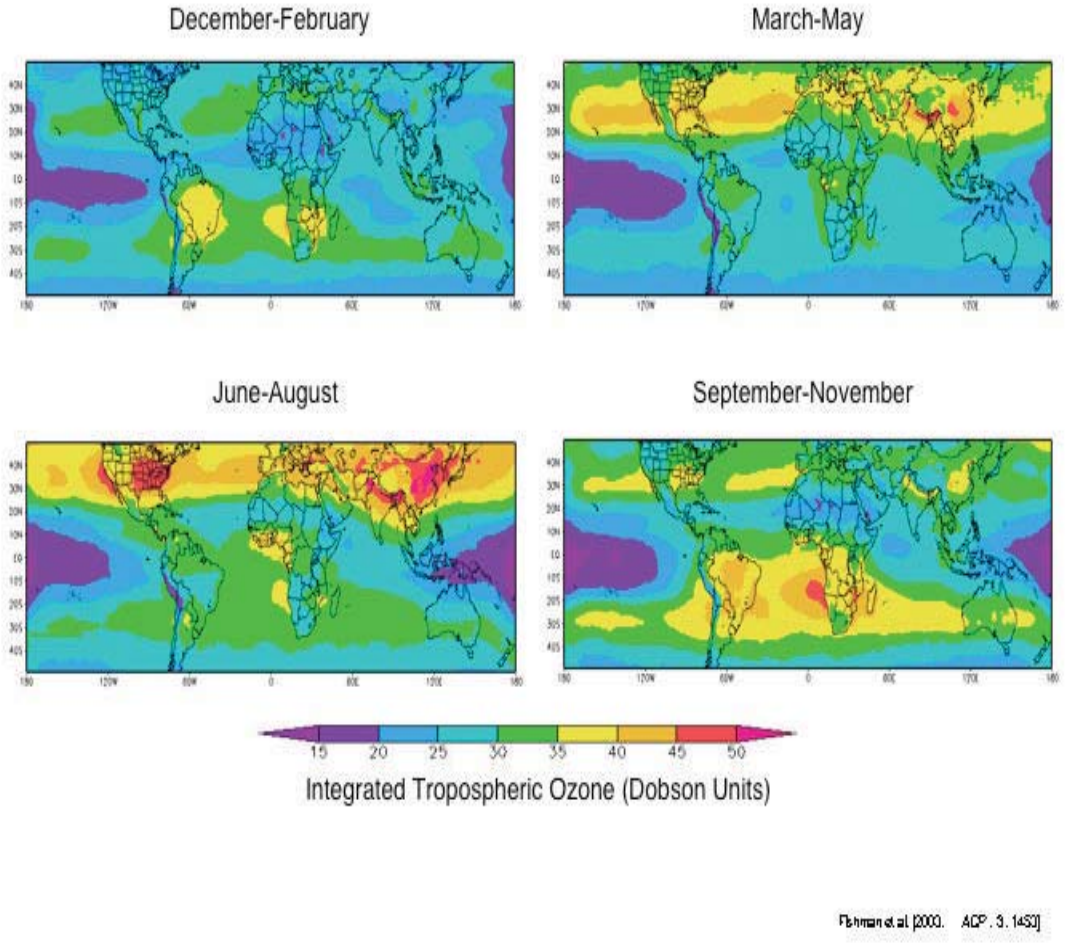

Figure 4. Climatological depiction of TOR (Fishman et al., 2003) using TOMS and SBUV measurements.

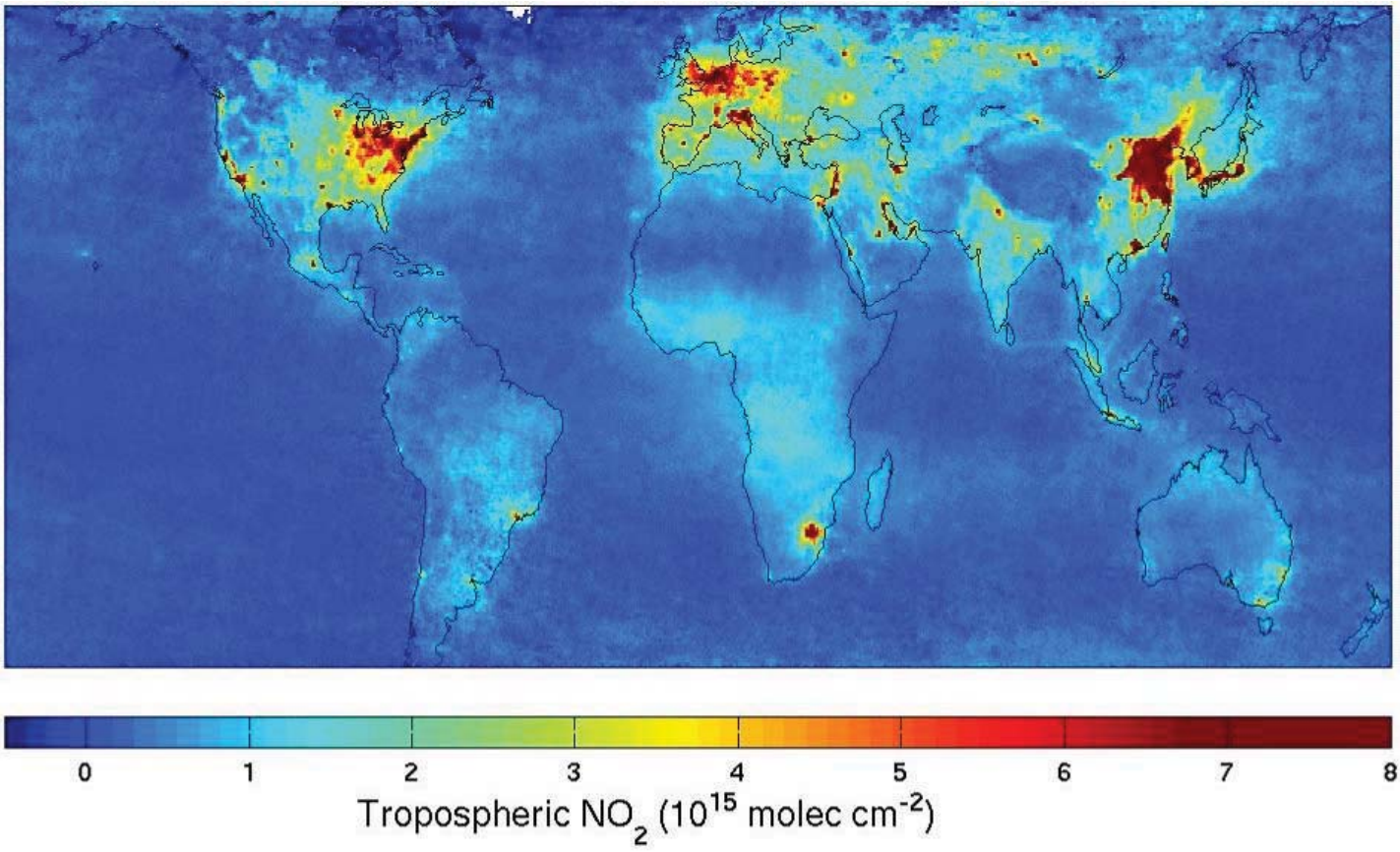

Figure 5. Tropospheric NO_2 columns retrieved by Martin et al. (2002) from the SCIAMACHY satellite instrument for 2004 –2005.

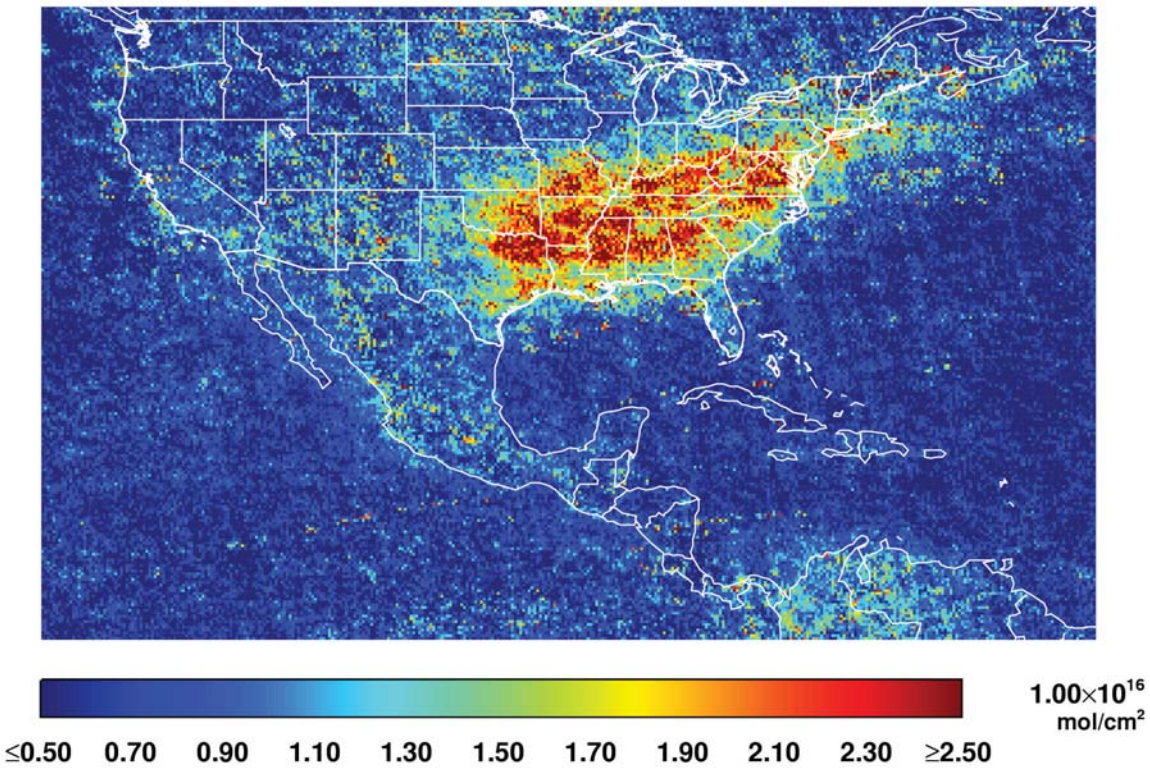

Figure 6. HCHO distribution of over eastern U.S. during August 2005.

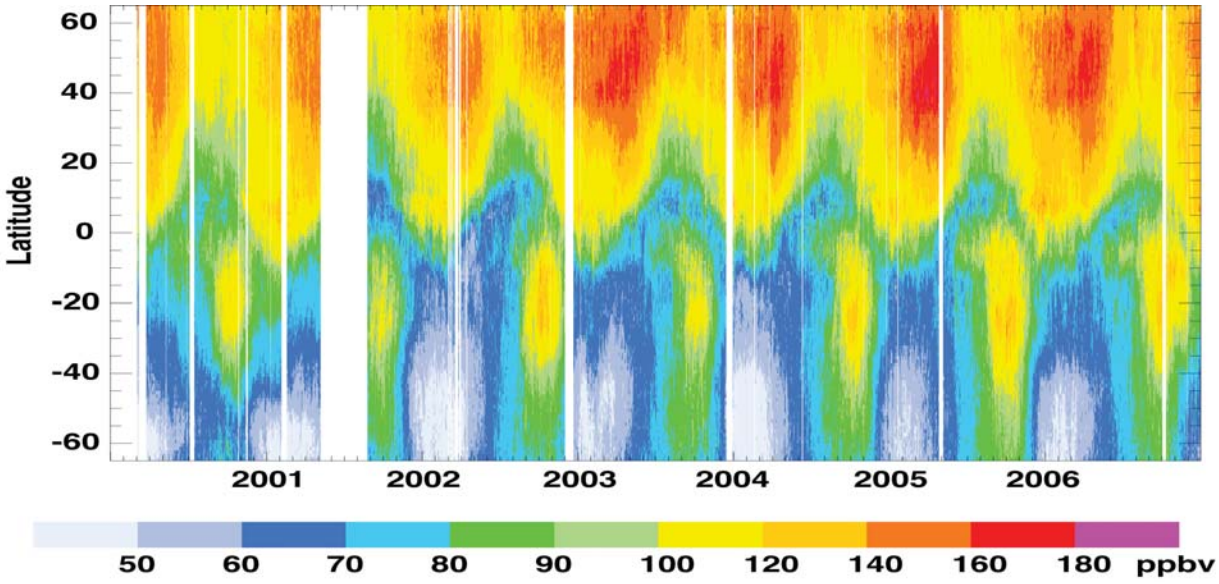

Figure 7. Zonal plot showing the CO 700 hPa mixing ratio at different latitudes over recent years. In the Southern Hemisphere, there is a large amount of CO emitted from agricultural fires in Africa and South America every year in the late summer. In the Northern Hemisphere, CO is produced by industry, urban activity and wildfires, and it is usually removed from the atmosphere by photochemistry during the summer. However, Western Russian fires in the late summer of 2002 and Siberian fires in the spring of 2003 produced so much CO that pollution built-up to produce a very "dirty winter."

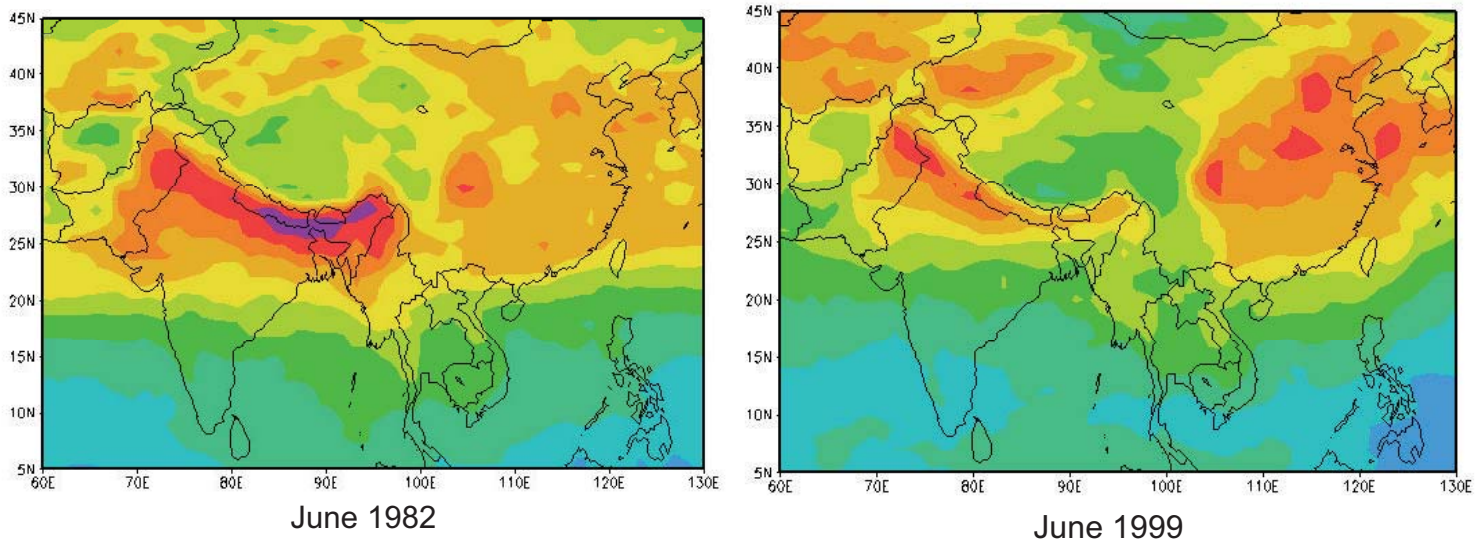

Figure 8. Monthly distributions of TOR in DU during June 1982 ("El Niño year) and June 1999 (La Niña year).

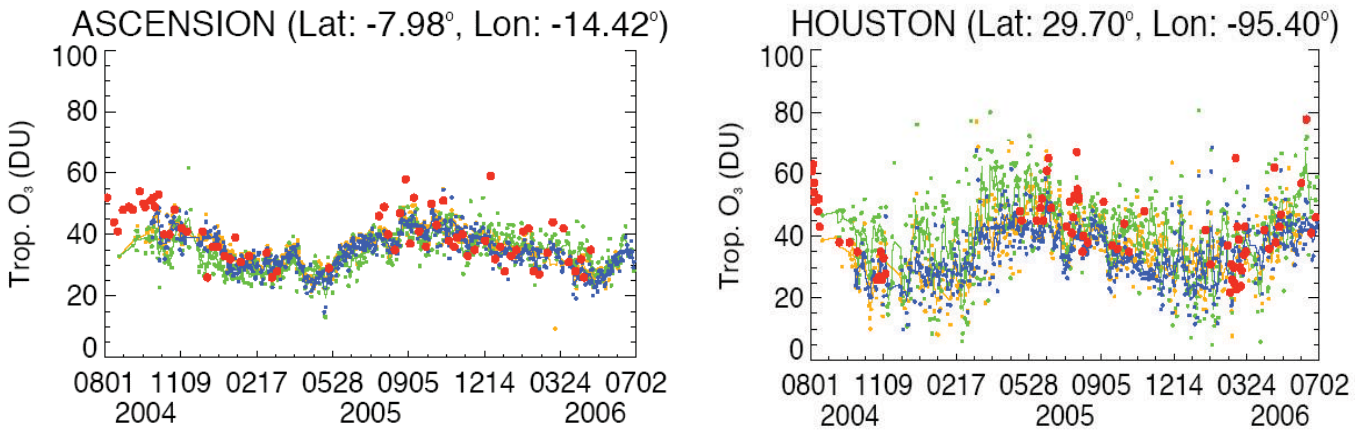

Figure 9. Time series comparisons of the three different TOR techniques compared to ozonesonde data integrated from the surface to the World Meteorological Organization (WMO) tropopause. Red circles indicate ozonesonde observations at each location. The various colored points connected by a running average line indicate the TOR calculated by various techniques: Ziemke et al., 2006 (yellow); Schoeberl (blue); and Fishman (green)

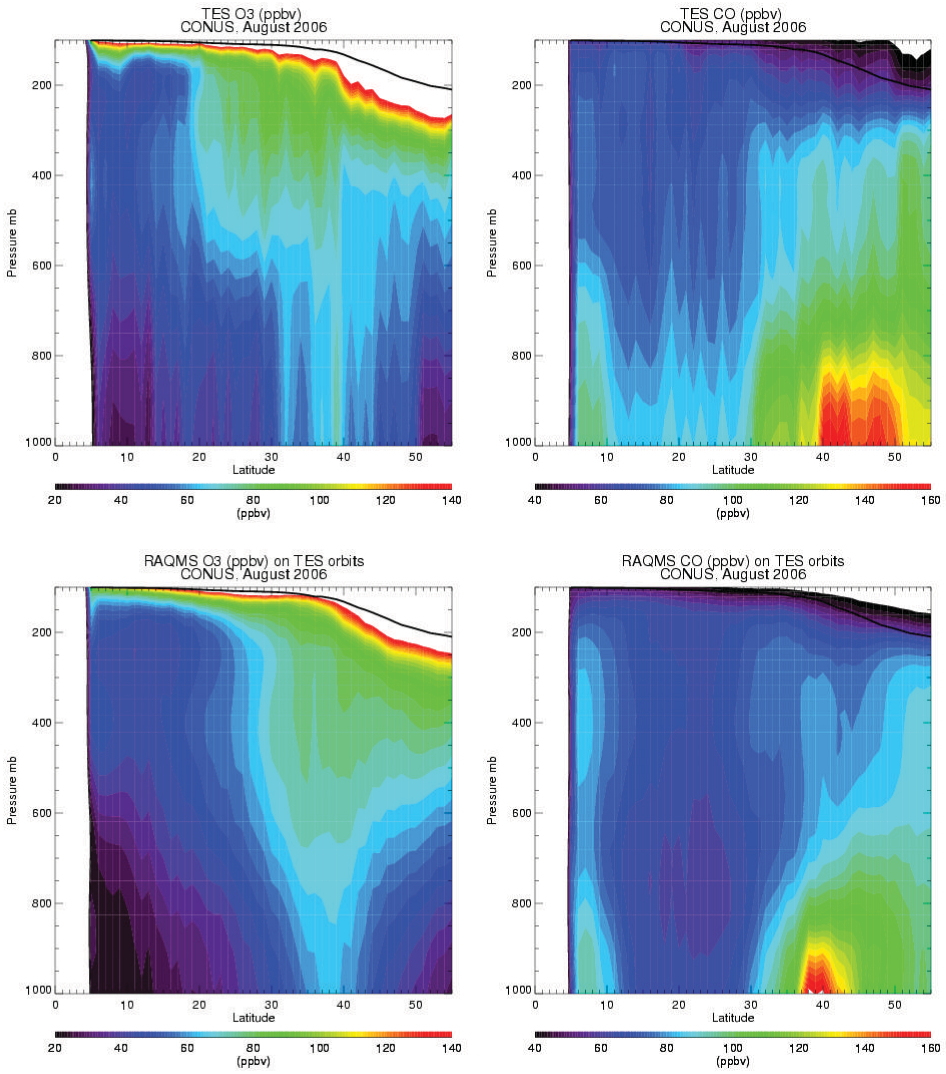

Figure 10. Composite distribution of O_3 and CO over the continental U.S. during August 2006 based on TES step and stare observations (upper panels) and RAQMS coincident chemical analyses (lower panels).

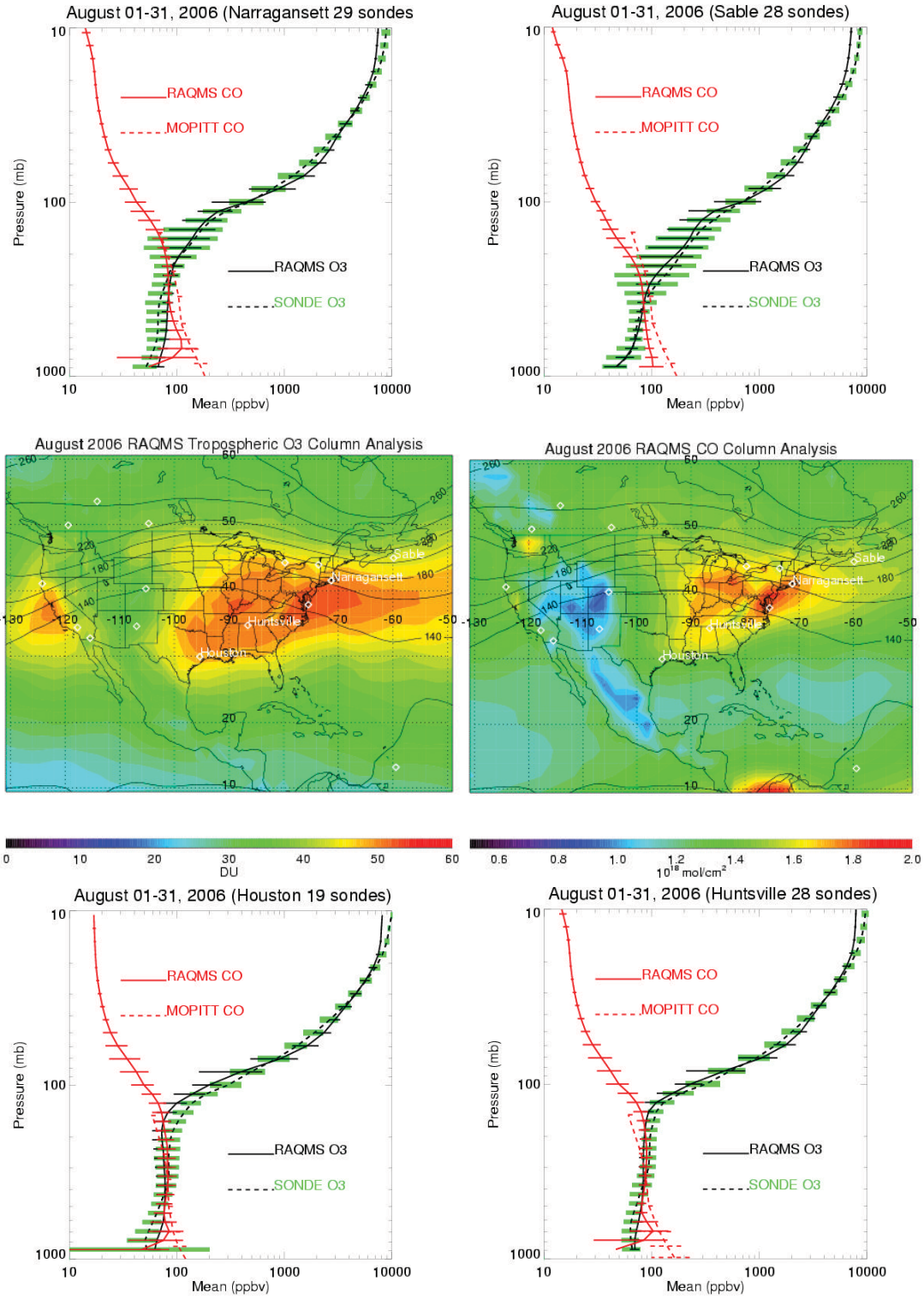

Figure 11. Mean distribution of O_3 and CO over the continental US during August 2006. Upper panels show comparisons for Narraganset and Sable Island IONS sites. Lower panels show

comparisons for Houston and Huntsville IONS sites. RAQMS (solid) and MOPITT (dashed) mean CO profiles and standard deviations are shown in red. RAQMS (solid) and IONS (dashed) mean O_3 profiles are shown in black. The IONS standard deviations are shown in green. The middle panels show the mean tropospheric column O_3 and total column CO based on six-hourly RAQMS analyses. The location of the IONS sites are indicated by white diamonds with the selected sites labeled. The mean pressure of the analyzed thermal tropopause is contoured.

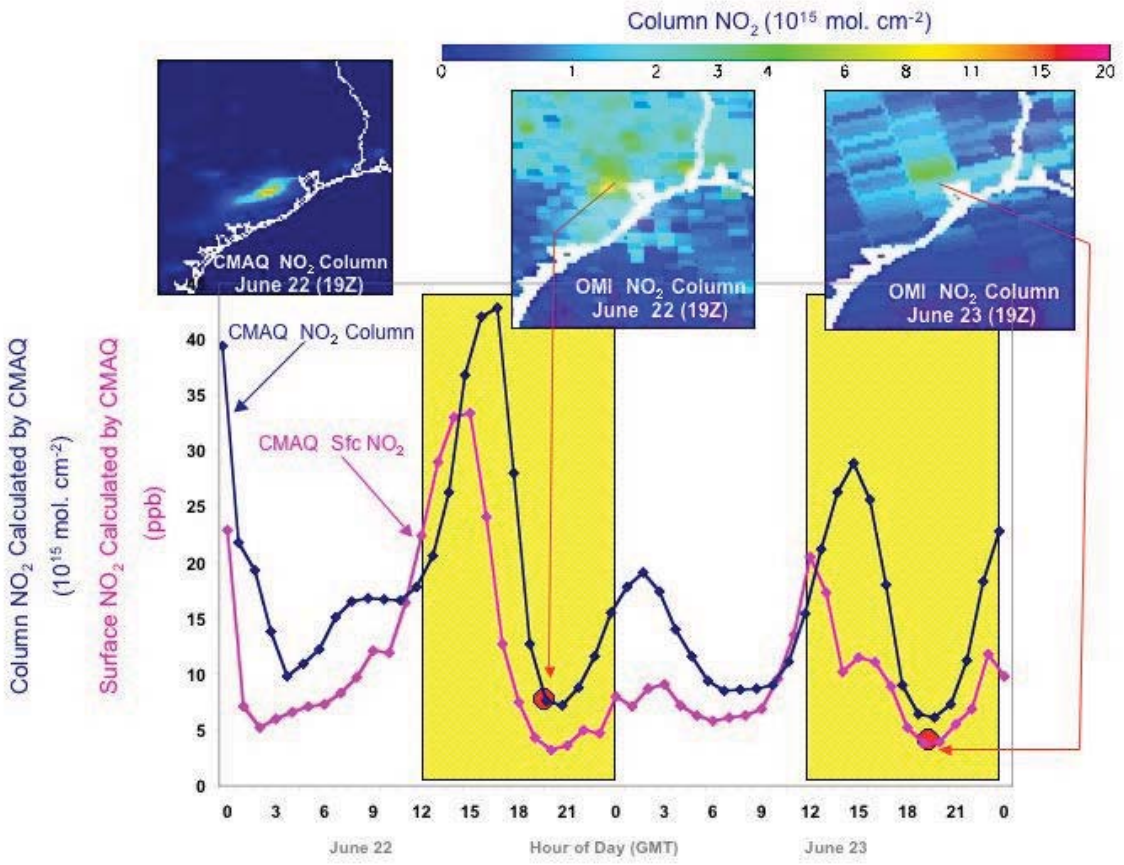

Figure 12. Two OMI NO_2 column measurements over Houston are depicted by the red circles at the time of the measurement (~1900 GMT) on June 22 and 23, 2005. The three depictions at the top portion of the figure are NO_2 column distributions: The left panel is calculated using CMAQ with a 12-km resolution; the other two panels are from OMI for the two respective days and all three depictions use the color scale above them. The diurnal calculations shown by the curves are the NO_2 surface concentrations (magenta) and the NO_2 columns (dark blue) calculated by the CMAQ model for Houston and are plotted hourly over this 2-day period. The yellow shading indicates daylight hours and illustrates when data using the solar backscattered technique (as used by OMI) could be obtained from a geostationary orbit.

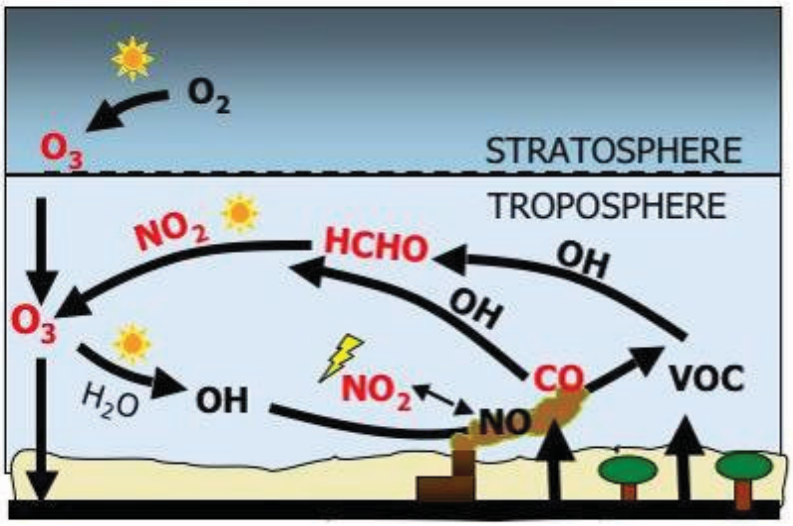

Sidebar Figure. Schematic diagram of simplified tropopsheric photochemistry. Species in red can be measured using existing satellite instrumentation. CO, NO and VOCs are emitted in the planetary boundary layer from both anthropogenic and biogenic sources. NO_2 is rapidly converted in the troposphere from emitted NO and the two nitrogen oxides (NO_x) establish an equilibrium ratio between each other depending on a number of atmospheric variables such as the intensity of sunlight and the amount of O_3. HCHO is an intermediate product of VOC oxidation, and its measurement is a good indication of the amount of VOCs present. The amount of O_3 produced is directly proportional to how much NO_2 is present when sunlight is available (denoted by the "sun" symbol). Ozone can also be transported to the troposphere from the stratosphere where it is produced naturally by the photolysis of molecular oxygen (O_2) because of high-energy photons in the upper atmosphere ($\lambda < 242$ nm) that are capable of breaking apart the O_2 molecule. Lightning is also a natural source of NO_x in the free troposphere.